International Journal of Technology (2016) 3: 424-430
ISSN 2086-9614

EFFECT OF PRESSURE IN POST-HYDROTHERMAL TREATMENT ON THE NANOSTRUCTURAL CHARACTERISTICS OF ZnO NANOPARTICLES

Akhmad Herman Yuwono[1,2*], Daniel Kurniawan[1], Nofrijon Sofyan[1,2], Ghiska Ramahdita[1,2] Amalia Sholehah[1,2]

[1]*Department of Metallurgical and Materials Engineering, Faculty of Engineering, Universitas Indonesia, Kampus UI Depok, Depok 16424, Indonesia*
[2]*Tropical Renewable Energy Center (TREC), Faculty of Engineering, Universitas Indonesia, Kampus UI Depok, Depok 16424, Indonesia*
[3]*Department Metallurgical Engineering, Faculty of Engineering, Universitas Sultan Ageng Tirtayasa, Jl. Jendral Sudirman Km 3, Cilegon-Banten 42435, Indonesia*

(Received: December 2015 / Revised: January 2016 / Accepted: February 2016)

ABSTRACT

Zinc Oxide (ZnO) is an important semiconductor material due to its broad applications, such as in the fields of electronics, optoelectronics, photocatalysts, and solar cells. The main purpose of this work was to investigate the effect of pressure in post-hydrothermal treatment on crystallinity enhancement, crystallite growth, and band gap reduction of ZnO nanoparticles, which could be expected to improve their performance as the semiconductor oxide layer in the dye-sensitized solar cell application. For this purpose, ZnO nanoparticles have been successfully synthesized through the precipitation method, followed by a sequence of thermal treatments including drying, calcination, and Post-hydrothermal Treatment (PHT). For increasing the crystallinity of ZnO nanoparticles, PHT was carried out with a pressure variation of 1 and 3 bar. The resulting nanoparticles were further characterized with X-Ray Diffraction (XRD), Ultra-Violet Visible (UV-Vis) spectroscopy and a Scanning Electron Microscope (SEM). The study showed that by increasing the PHT pressure from 1 to 3 bar caused an adverse effect on the crystallinity, *i.e.* the crystallite size of ZnO nanoparticles slightly decreased from 27.42 to 26.88 nm. This was expected to be due to the increase of the boiling point of water causing less effective of vapor generated to improve the crystallinity by a cleavage mechanism on the inorganic framework. The band gap energy (E_g), however, was found to increase slightly from 3.25 to 3.26 eV, respectively. Considering the obtained properties, ZnO nanoparticles in this study have the potential to be used as the semiconductor oxide layer in the dye-sensitized solar cells.

Keywords: Bandgap; Crystallinity; Crystallite size; Post-hydrothermal treatment; ZnO nanoparticles

1. INTRODUCTION

In recent years, semiconductor nanomaterials, due to their novel properties over their bulk properties, have received significant attention from worldwide researchers and industry communities (Srivastava et al., 2013). Zinc oxide (ZnO) is one of important materials which has been gaining special attention for various strategic applications, including solar energy to

*Corresponding author's email: ahyuwono@eng.ui.ac.id Tel. +62-21-7863510, Fax. +62-21-7872350
Permalink/DOI: http://dx.doi.org/10.14716/ijtech.v7i3.2990

electrical conversion in dye-sensitized solar cell devices, photocatalysts, and optoelectronics (Kołodziejczak-Radzimska & Jesionowski, 2014; Yuwono et al., 2010). Various methods have been used to synthesize ZnO nanoparticles, such as precipitation (Srivastava et al., 2013), sol-gel (Yuwono et al., 2010), hydrothermal (Wen et al., 2014), and chemical bath deposition (Sholehah et al., 2013). In these previous studies, ZnO nanoparticles were synthesized using the precipitation method, considering its low cost and high purity level of the resulting product. Even so, agglomeration is most likely to happen because of the high overall surface energy causing a low crystallinity level, hence it results in non-optimal optical properties, including low level photon absorption (Wang, 2004). Additionally, Yuwono et al. (2010; 2013) have made an effort to improve the crystallinity of TiO_2 and ZnO nanoparticles using post-hydrothermal treatment (PHT), which is a water vapor treatment to break down the agglomeration and rearrange the inorganic framework of nanostructured materials, resulting in a much greater crystallinity. Based on their research, an increase in temperature of the post-hydrothermal treatment has been found to increase the crystallinity of nanoparticles. However, in their previous study, the pressure of the system was not investigated yet. In fact, the crystallinity enhancement on nanoparticles by this post-hydrothermal treatment not only contributed to the increase of temperature, but also by pressure, according to the ideal gas law.

In the present work, post-hydrothermal treatment (PHT) was carried out with a pressure variation of 1 and 3 bar, which is specifically aimed at investigating the effect of pressure in post-hydrothermal treatment on the crystallinity enhancement, crystallite growth, and band gap reduction of ZnO nanoparticles, which can be expected to improve their performance as the semiconductor oxide layer in the dye-sensitized solar cell application.

2. EXPERIMENTAL METHODS

The ZnO nanoparticles in this study were synthesized through the precipitation method. The precursors used in this study were a zinc acetate and lithium hydroxide solution. A solution of 0.1 M $Zn(CH_3COO)_2$ and 0.2 M LiOH was prepared by dissolving 2.2 gr $Zn(CH_3COO)_2.2H_2O$ (Sigma-Aldrich) and 0.48 gr LiOH (Merck) in ethanol absolute (Merck), respectively. The dried precipitate was ground and washed with warm distilled water (45°C) and moreover, dried again in a standard oven (Memmert, Germany). Subsequently, the dried ZnO nanoparticles were calcined in a tube furnace at 300°C for 2 hours, and then they were post-hydrothermally treated in a pressurized autoclave at 1 and 3 bar, at 100°C for 1 hour. The crystallinity and crystallite size of ZnO nanoparticles were characterized by X-Ray Powder Diffraction (XRD), while the band gap energy of ZnO nanoparticles were characterized by Diffuse Reflectance Spectroscopy (DRS), and a Field Emission-Scanning Electron Microscopy (FEI, FE-SEM) was used to examine the morphology and particle size of the nanoparticles.

3. RESULTS AND DISCUSSION

XRD traces of as-synthesized (O), as-washed (W), as-calcined (C), and as post-hydrothermally treated (H1 and H3) ZnO nanoparticles are shown in Figure 1. All the diffraction peaks of the samples can be indexed as wurtzite ZnO by ICDD PDF-2 Files No. 01-080-0075, except for the as-synthesized one. The as-synthesized ZnO was still dominated by the impurities phase, *i.e.* lithium acetate from the precursor. It was only after washing that the XRD pattern showed a pure crystalline phase of ZnO. According to Figure 1, the intensity of ZnO peaks increases with a further thermal treatment by calcination and post-hydrothermal treatments, indicating a significant increase in crystallinity. Prior to PHT, indeed it is clearly shown that there was a ghost peak of the lithium acetate in the sample, which was then removed by water vapor treatment, thus causing the lithium acetate to dissolve in water.

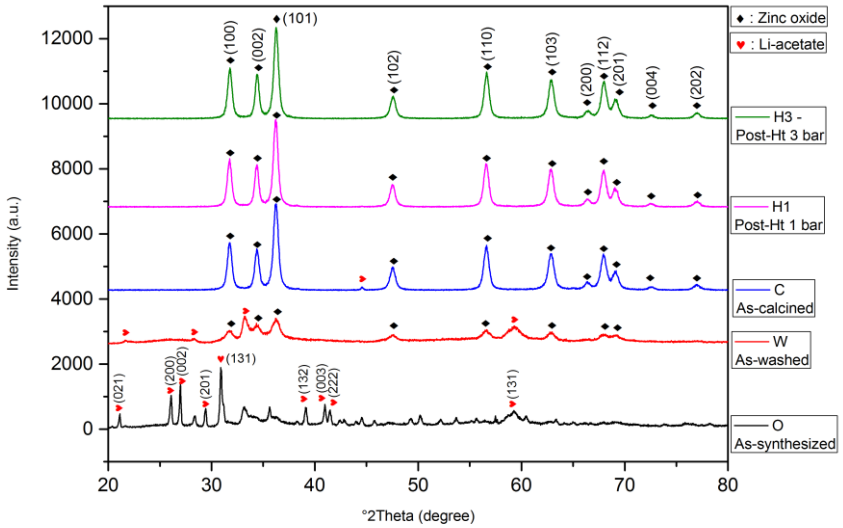

Figure 1 XRD traces of ZnO nanoparticles: as-synthesized (O); as-washed (W); as-calcined (C); as post-hydrothermally treated at 1 bar (H1) and 3 bar (H3)

The line broadening from the XRD peaks is apparently shown by the ZnO samples in this study, indicating that the resulting crystallites are in the nanometer scale. The average crystallite size of nanoparticles was calculated by using Scherrer's equation, as shown in Equation 1:

$$t = \frac{k\lambda}{B\cos\theta} \tag{1}$$

where t is the average crystallite size; k is Scherrer constant (0.89 for spherical particle); λ is wavelength of CuK_α (1.54056 Å); B is the broadening or full-width at half-maximum (FWHM) in radiant; and θ is the Bragg diffraction angle. It should be noted that the broadening due to instrument and strain has been excluded in this investigation, and the estimated average crystallite size of the ZnO samples is presented in Table 1.

Table 1 Comparison of average crystallite size of ZnO nanoparticles

Sample code	Average crystallite size (nm)
As-washed (W)	7.37
As-calcined (C)	24.48
Post-hydrothermally treated at 1 bar (H1)	27.42
Post-hydrothermally treated at 3 bar (H3)	26.88

From Table 1, it can be seen that the as-washed sample (W) has the smallest average crystallite size, i.e. 7.37 nm. A significant crystallinity enhancement was obtained after the calcination process, increasing the crystallite size up to 24.48 nm. In this context, the thermal energy facilitated ZnO nanoparticles to grow through the Ostwald ripening phenomenon, where smaller particles diffuse into each other to create much larger particles (Cao, 2004). A further crystallinity enhancement was obtained by the application of post-hydrothermal treatment at 1 bar (H1) up to 27.42 nm. However, a further increase in pressure of the process up to 3 bar (H3)

did not contribute to a greater crystallite size, even though there was a slightly reduction down to 26.88 nm. This can be likely due to a bigger pressure applied in the process that has increased the boiling point of water, causing less effective vapor generated to improve the crystallinity of ZnO nanoparticles by cleavage. Therefore, it can be concluded from this result that while increasing temperature in the post-hydrothermal treatment can enhance the nanocrystallinity significantly, increasing the pressure did not produce the same results for the crystallinity enhancement.

The diffuse reflectance spectrascopy (DRS) of as-washed, as-calcined, and PHT ZnO nanoparticles are shown in Figure 2. The as-washed sample shows a good reflectance at wavelength longer than 400 nm, while the as-calcined and PHT samples are red-shifted to 430 nm. This can be most likely attributed to the agglomeration of ZnO nanoparticles (as shown later by SEM results in Figure 3c), (Kumar et al., 2013). The band gap energy (E_g) of ZnO nanoparticles was estimated through extrapolation of the linear portion of the graph, using the Kubelka-Munk function (Morales et al., 2007), which is presented in Figure 2b.

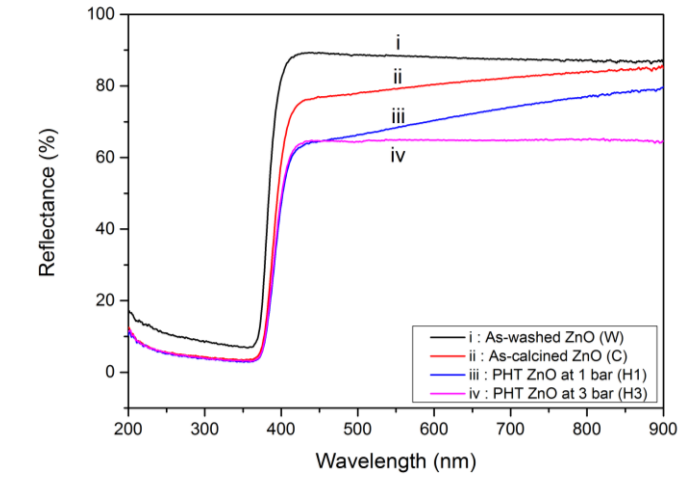

(a)

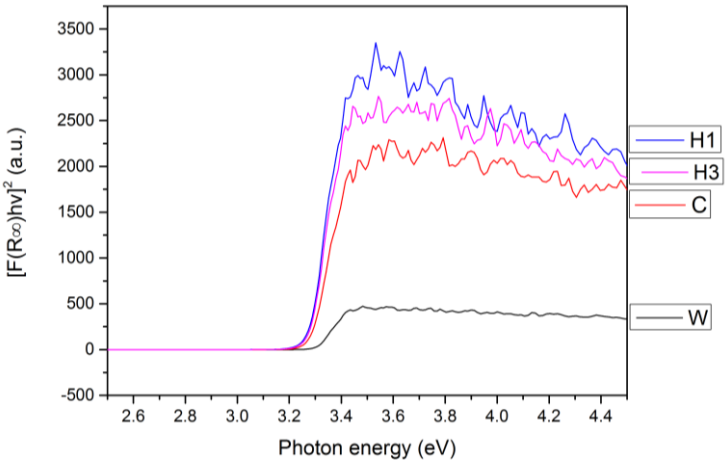

(b)

Figure 2 DRS spectra of ZnO nanoparticles: (a) before Kubelka-Munk transformation; (b) after Kubelka-Munk transformation

Through this procedure, the estimated band gap energy (E_g) of the as-washed ZnO is 3.29 eV, as-calcined ZnO is 3.26 eV, and PHT at 1 and 3 bar ZnO are 3.25 and 3.26 eV, respectively.

The crystallite growth of each samples contributes to this reduction in band gap energy, which is consistent with the results of estimated crystallite size calculation in Table 1. This is due to the quantum confinement effect, a phenomenon that occurs when the crystallite size is small enough i.e., below the Bohr radius of the exciton pair, which is around 1-10 nm. The band gap energy increases because of the potential barrier or vice versa, i.e., the band gap decreases when the crystallite grows bigger at the nanometer scale (Poole Jr. & Owens, 2003).

Figure 3 shows the FE-SEM images of the synthesized ZnO particles. In general, the resultant ZnO phase appeared as a 'flakes' morphology (Figures 3a and 3b). After calcination, the microstructure shows a more spherical particle morphology, as can be seen in Figures 4a and 4b. This might be attributed to the agglomeration of acetate precursors in as-synthesized ZnO. The particle size of as-washed ZnO is rather large, which is 60 to 80 nm, due to the high agglomeration level (Wang, 2004), while the as-calcined and PHT ZnO show relatively smaller particle sizes, which are in the range of 27 to 44 nm in diameter.

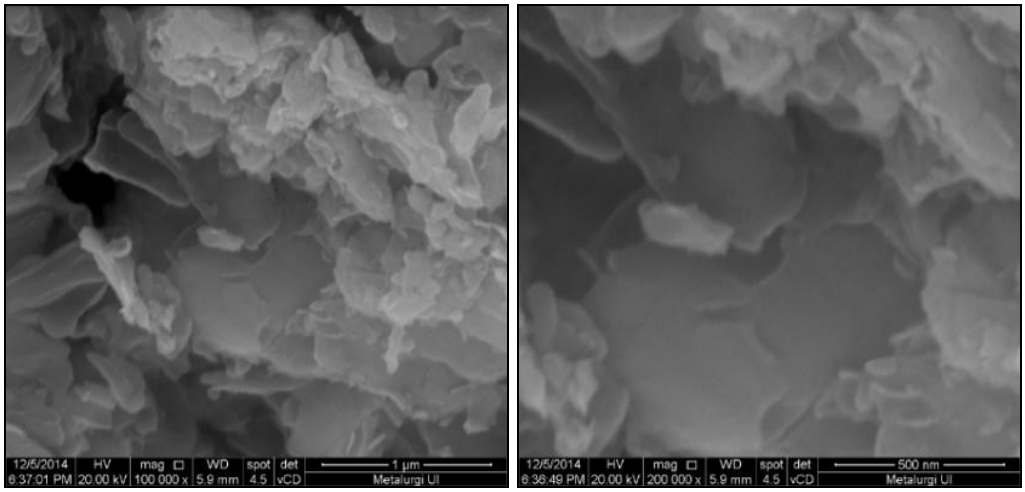

(a) (b)

Figure 3 Secondary electron images of the as-synthesized ZnO nanoparticles at two different magnifications with (a) a scale bar of 1 µm; and (b) a scale bar of 500 nm

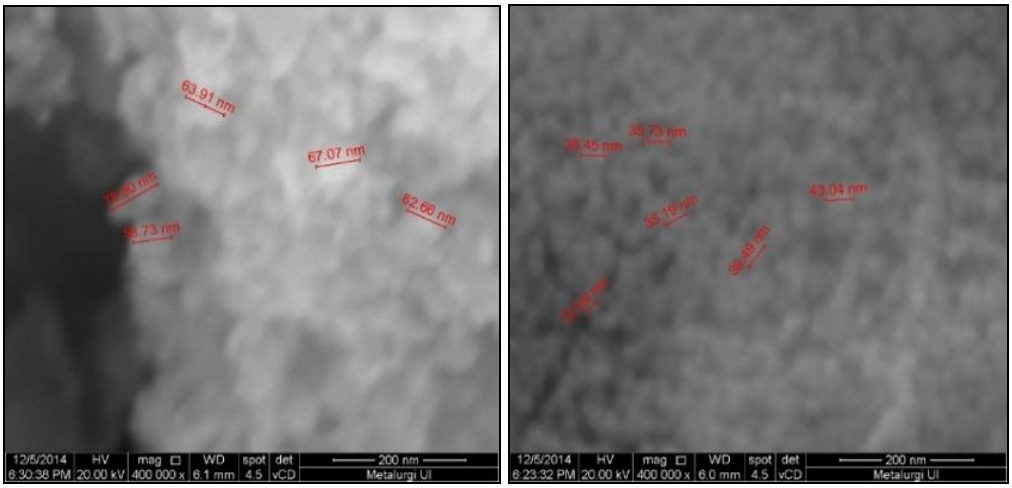

(a) (b)

Figure 4 Secondary electron images of the as-washed (a) and as-calcined (b) ZnO nanoparticles

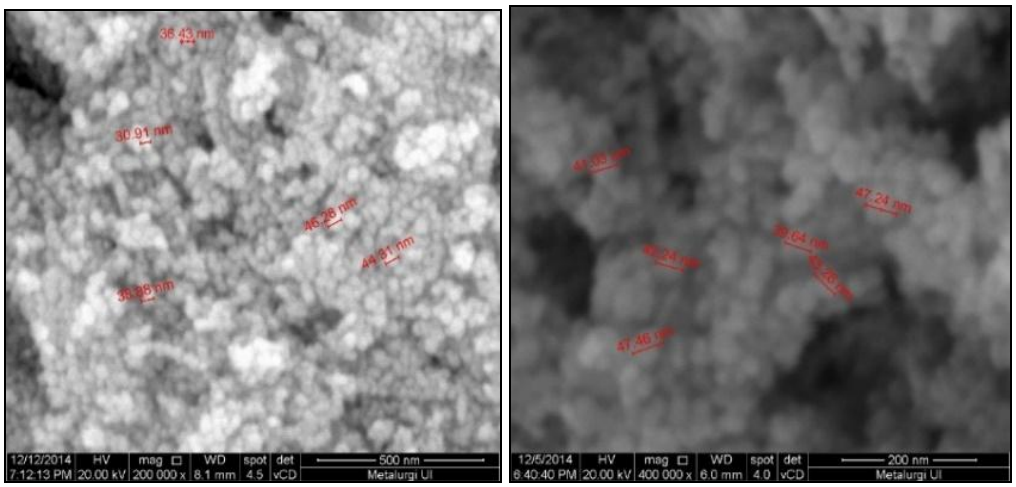

(a) (b)

Figure 5 Secondary electron images of the post-hydrothermal ZnO nanoparticles at: (a) 1 bar; and (b) 3 bar

Secondary electron images of the post-hydrothermal ZnO nanoparticles at different pressures can be seen in Figure 5. Furthermore, Figure 5a shows the morphology at 1 bar, whereas Figure 5b shows the morphology of nanoparticles at 3 bar. As can be seen in this figure, an increase in pressure from 1 bar to 3 bar does not lead to the expected result in crystallinity improvement, even when an adverse effect has occurred, *i.e.* the particle size is slightly smaller than that of 1 bar. This could be due to high pressure that was applied in the post-hydrothermal treatment in which high pressure would increase the boiling point of water, resulting in a less effective amount of vapor generated to improve the crystallinity by the cleavage mechanism on the inorganic oxide phase network.

4. CONCLUSION

The investigation results showed that the precipitation technique used to synthesize ZnO nanoparticles in this study has produced nanoparticles with an average crystallite size of 7.37 nm and band gap of 3.29 eV for as-washed ZnO. A significant crystallite growth can be achieved by calcination, which resulted in the crystallite size up to 24.48 nm and band gap energy reduction to 3.26 eV. The pressure-controlled post-hydrothermal treatment at 1 bar could provide a slight increase in crystallite growth to 27.42 nm, and a decrease of band gap energy to 3.25 eV. However, an increase in pressure to the higher level of 3 bar did not lead to the expected result in crystallinity improvement, even when an adverse effect occurred, *i.e.* the particle size of 3 bar was slightly smaller than that of 1 bar. This was expected to be due to high pressure that was applied in the post-hydrothermal treatment in which high pressure would increase the boiling point of water, resulting in a less effective amount of vapor generated to improve the crystallinity by the cleavage mechanism on the inorganic oxide phase network. The similar band gap of as-calcined and post-hydrothermally treated ZnO may result, due to the brief holding time, hence producing a slower rate of crystallinity enhancement.

5. ACKNOWLEDGEMENT

The authors are grateful for the main financial support from Ministry of Research and Higher Education-Republic of Indonesia through the Decentralization-PUPT Research Grant 2015, coordinated by the Directorate of Research and Community Services-Universitas Indonesia (DRPM-UI) with Contract No. 0549/UN2.R12/HKP.05.00/2015. Partial support from the Start-Up Research Grant of Tropical Renewable Energy Center (TREC) Faculty of Engineering

Universitas Indonesia with Contract No. 1212/UN2.F4.D/HKP.05.00/2015 is also acknowledged.

6. REFERENCES

Cao, G., 2004. *Nanostructures and Nanomaterials*. Imperial College Press, London

Kołodziejczak-Radzimska, A., Jesionowski, T., 2014. Zinc Oxide—From Synthesis to Application: A Review. *Materials*, Volume 7, pp. 2833–2881

Kumar, S.S., Venkateswarlu, P., Rao, V.R., Rao, G.N., 2013. Synthesis, Characterization and Optical Properties of Zinc Oxide Nanoparticles. *Int. Nano Lett*., Volume 3, pp. 1–6

Morales, A.E., Mora, E.S., Pal, U., 2007. Use of Diffuse Reflectance Spectroscopy for Optical Characterization of un-supported Nanostructures. *Rev. Mex. Fisica*, Volume 53, pp. 18–22

Poole Jr., C.P., Owens, F., 2003. *Introduction to Nanotechnology*. John Wiley & Sons, Inc., Hoboken, New Jersey

Sholehah, A., Yuwono, A.H., Poespawati, N.R., Trenggono, A., Maulidiah, F., 2013. High Coverage ZnO Nanorods on ITO Substrates via Modified Chemical Bath Deposition (CBD) Method at Low Temperature. *Adv. Mater. Res*., Volume 789, pp. 151–156

Srivastava, V., Gusain, D., Sharma, Y.C., 2013. Synthesis, Characterization and Application of Zinc Oxide Nanoparticles (n-ZnO). *Ceram. Int.*, Volume 39, pp. 9803–9808

Wang, Z.L., 2004. Zinc Oxide Nanostructures: Growth, Properties, and Applications. *J. Phys.: Condens. Matter* Volume 16, pp. R829–R858

Wen, J., Hu, Y., Zhu, K., Li, Y., Song, J., 2014. High-temperature-mixing Hydrothermal Synthesis of ZnO Nanocrystals with Wide Growth Window. *Curr. Appl. Phys*., Volume 14, pp. 359–365

Yuwono, A.H., Munir, B., Ferdiansyah, A., Rahman, A., Handini, W., 2010. Dye-sensitized Solar Cell with Conventionally Annealed and Post-hydrothermally Treated Nanocrystalline Semiconductor Oxide TiO¬2 derived from Sol-gel Process. *Makara Teknologi*, Volume 14, pp. 53–60

Yuwono, A.H., Sholehah, A., Harjanto, S., Dhaneswara, D., Maulidiah, F., 2013. Optimizing the Nanostructural Characteristics of Chemical Bath Deposition derived ZnO Nanorods by Post-hydrothermal Treatments. *Adv. Mater. Res*., Volume 789, pp. 132–137